Applied Energy 193 (2017) 139–148

Contents lists available at ScienceDirect

Applied Energy

journal homepage: www.elsevier.com/locate/apenergy

Stochastic model of wind-fuel cell for a semi-dispatchable power generation

Fernanda Alvarez-Mendoza [a,*], Peder Bacher [b], Henrik Madsen [b], César Angeles-Camacho [a]

[a] Instituto de Ingeniería UNAM, Universidad Nacional Autónoma de México, Mexico
[b] DTU Compute, Technical University of Denmark, Denmark

HIGHLIGHTS

- Semi-dispatchable generation based on time series analysis.
- Hybrid system for distributed generation with zero frequency and voltage instability.
- Hybrid system management implementing model predictive control.
- Short-term forecast to create power generation trajectory.

ARTICLE INFO

Article history:
Received 9 November 2016
Received in revised form 10 February 2017
Accepted 11 February 2017
Available online 20 February 2017

Keywords:
Distributed generation
Forecast
Energy intermittence
Model predictive control
Fuel cell
Hydrogen

ABSTRACT

Hybrid systems are implemented to improve the efficiency of individual generation technologies by complementing each other. Intermittence is a challenge to overcome especially for renewable energy sources for electric generation, as in the case of wind power. This paper proposes a hybrid system as an approach for reducing and overcoming the volatility of wind power, by implementing storage technology, forecasts and predictive control. The proposed hybrid system, which is suitable for the distributed generation level, consists of a wind generator, an electrolyzer, hydrogen storage and a polymer electrolyte membrane fuel cell, which are embedded in one complete system with the wind power. This study uses historic wind speed data from Mexico; the forecasts are obtained using the recursive least square algorithm with a forgetting factor. The proposed approach provides probabilistic information for short-term wind power generation and electric generation as the outcome of the hybrid system. A method for a semi-dispatchable electric generation based on time series analysis is presented, and the implementation of wind power and polymer electrolyte membrane fuel cell models controlled by a model predictive control approach is developed.

1. Introduction

Renewable energies are increasingly being used to generate electricity. Integration to the network, however, requires adjusting the new technologies in order to meet the established norms. Wind and photovoltaic renewable energy generation technologies are up to now the most developed and, in both, intermittence is the major issue to attend for connection to the grid.

Studies concerning non-dispatchable generation combined with storage which focus on isolated networks are [1–3] where a DC configuration is proposed for the renewable energy integration and storage is implemented to increase the use of wind power and reduce the operation of backup systems. For stand-alone systems employing two or more technologies to generate electricity is common.

Another way to deal with intermittence is to combine the wind power generation with the forecast, in order to more accurately plan how to use the generated power and how to participate in market regulation [4,5]. The wind power uncertainty has been another research topic as in [6] where wind power forecasting uncertainty is investigated in the unit commitment. The study of levelized costs of grid-connected wind turbines with energy storage device (ESD) [7,8] or renewable sources implemented as distributed generation (DG) [9], as well as the analysis of the wind energy in Germany [10], are examples of the many studies in the implementation of renewable energies.

The issue with intermittence in wind power can be decreased when a forecast model is implemented. The approach suggested in this study uses an ESD to stabilize the inherent variations and

* Corresponding author.
E-mail address: malvarezm@iingen.unam.mx (F. Alvarez-Mendoza).

http://dx.doi.org/10.1016/j.apenergy.2017.02.033
0306-2619/

Nomenclature

E	open circuit voltage
F	Faraday constant
H	hydrogen
H_{2used}	volume of hydrogen required by the FC
I	current
l	impulse response
M	number of points in average filter
N	future outputs for a horizon
n	number of cells
O	oxygen
p	ambient pressure
P	active power
P_{el}^{nom}	electrolyzer nominal power
P_{fc}^{nom}	fuel cell nominal power
P_{t+k}^{ref}	power reference trajectory
$\widehat{P}_{t+k}^{w}$	forecasted wind power
P_o	balance power
P_w	actual and forecasted wind power
P_ϕ	power flow to/from storage elements
P_{elmax}	activation vector of electrolyzer
P_{el}	electrolyzer power
P_{fcmax}	activation vector of FC
P_{fc}	fuel cell power
R	ideal gas constant
T	temperature
t	time
V	voltage
V_c	cell voltage
V_g	gas volume
V_{act}	activation voltage
V_{H_2}	volume of hydrogen
V_{ohm}	ohmic voltage
V_{trans}	transport voltage
X	matrix of past observations
Y_{t+1}	forecast one step ahead
Y_t	historic data
z	number of excess electrons

Greek

Δt	age of the data
Γ_{el}	threshold of low level percent of storage
Γ_{fc}	threshold of min percent of storage for FC
λ	forgetting factor
μ	correction for the mean value
ω	weight
ϕ	storage level
ϕ_0	last value of storage level
Θ	weight of past observations
θ	vector of weight of past observations
ε	white noise

to balance the deviations of the actual wind power to better meet the planned network infeed. The purpose of the ESD is to reduce the intermittence with the implementation of a filter and to be able to meet the short-term planned production of the hybrid system (HS) at the distribution level. To keep a stable frequency in the network, what matters for the operation of the transmission system is not so much the variation in production but the unpredictability of the production which is study in this work.

The major contribution in this paper, as shown in the following sections, is the ability to change the output power of the HS from a non-dispatchable to a semi-dispatchable generation giving the capability to inform the independent system operator (ISO) to program the network dispatch. The flexibility of power dispatch depends greatly on the short-term prediction and the storage characteristics to reduce the variations of the power generated by the wind turbine.

Unlike other studies, this paper proposes an advance energy management system (AEMS) to overcome the effect on the frequency when the HS, relying solely on clean energy sources without depending on fossil power plants, is connected as DG.

2. Implemented models

The sample size of historic data implemented in the forecast model was given by measurements over a period of three months with a resolution of 10 min.

2.1. Forecast model

Energy forecasting is particularly meaningful when considering wind power because of the cost relation, dispatch planning and market operations [11], the focus in this paper is dispatch planning.

The sample data used for the forecast was given by a three months with a resolution of 10 min (12,960 measurements) but the complete study was made for a whole year. Even though the collected measurements data covers a year, in this study only the first week of results was shown so the reader can truthfully see the behavior of the hybrid system and the output power in a clear way.

2.1.1. Autoregressive model

In this model, the current value of the process was expressed as a finite, linear aggregate of previous values of the process. The AR model is a classic forecast model implemented in time series analysis. An AR(ρ) model relates ρ historic observations to the value Y_{t+1}

$$Y_{t+1} = \mu + \sum_{i=0}^{\rho-1} \Theta_i Y_{t-i} + \varepsilon_{t+1} \tag{1}$$

$$Y_{t+1} = \hat{Y}_{t+1|t} + \varepsilon_{t+1} \tag{2}$$

from Eq. (1), μ is a term correcting the mean value, Θ_i is the coefficient of each past observation Y_{t-i} describing its influence on the next value Y_{t+1}, and finally ε_t is assumed to be white noise [12,13]. This is an iterative process, meaning that a six-steps-ahead forecast is required to calculate (2), to upgrade Y_t plugging in the last forecast value generated, and to repeat the process:

$$\hat{Y}_{t+k|t} = \mu + \sum_{i=0}^{\rho-1} \hat{\theta}_i \hat{Y}_{t+k-(i+1)|t} \tag{3}$$

$\hat{Y}_{t+k-(i+1)|t}$ is equal to the observation if the observation exists; otherwise, it is equal to the prediction. An AR process is a linear process characterized by a finite number of terms.

2.1.2. Recursive least square with forgetting factor [14]

Notice that the k-step AR(ρ) model can be written as

$$Y_{t+k} = (Y_t, Y_{t-1}, \ldots, Y_{t-\rho+1}) \begin{pmatrix} \Theta_0 \\ \vdots \\ \Theta_{\rho-1} \end{pmatrix} + \varepsilon_{t+k} \quad (4)$$

which, by introducing the standard notation using X as the regressor vector, becomes

$$Y_{t+k} = X_t^T \hat{\theta}_t + \varepsilon_{t+k}. \quad (5)$$

RLS with forgetting factor is based on the AR process and allows the parameter vector θ to change over time. For the weighted least squares estimator, the weighted estimation is calculated as

$$\hat{\theta}_t = \hat{\theta}_{t-1} + R_t^{-1} X_{t-k} \left[Y_t - X_{t-k}^T \hat{\theta}_{t-1} \right] \quad (6)$$

where

$$R_t = \lambda R_{t-1} + X_{t-k} X_{t-k}^T \quad (7)$$

this is a recursive implementation of a weighted least squares estimation, where the weights are exponentially decaying over time. With X_t as the regressor vector, θ_t as the coefficient vector and Y_t as the dependent variable (observation at time t), the k-step prediction at t is

$$\hat{Y}_{t+k|t} = X_t^T \hat{\theta}_t \quad (8)$$

the parameter λ is the forgetting factor, describing how fast historical data are down-weighted. The weights are equal to

$$\omega(\Delta t) = \lambda^{\Delta t} \quad (9)$$

Δt is the age of the data [15]. Typical values for λ are in the range from 0.90 to 0.995. The forgetting factor can be chosen based on assumptions of the dynamics, or it can be a part of the global optimization [14].

2.2. Electrolyzer model

In order to implement a controller one must understand and describe the dynamical system. Therefore, in this and the following section the basic operation of the electrolyzer and the fuel cell will be introduced.

The basic operation of the electrolyzer can be demonstrated by a small experiment, which is shown in Fig. 1 [16]. The water is electrolyzed into hydrogen and oxygen by passing an electric current through it.

The electrolysis is fundamental for the production of pure hydrogen, and this must be taken into account in the hybrid system model, by implementing the laws of Faraday electrolysis.

Faraday's first law of electrolysis. The mass of the substance altered at the electrode during the electrolysis is directly proportional to the amount of electricity transferred to that electrode. The quantity of electricity indicates the amount of electrical charge, typically measured in coulombs [17].

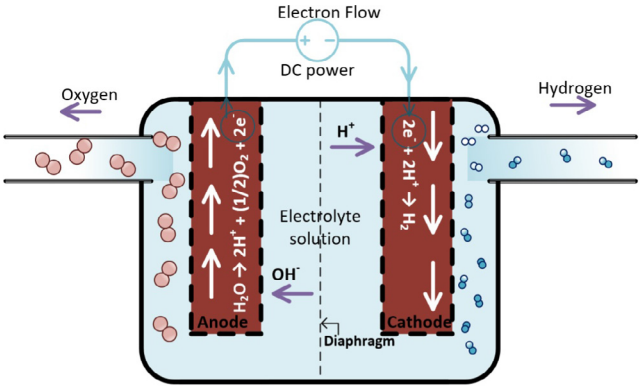

Fig. 1. Water electrolysis experiment.

Faraday's second law of electrolysis. When the same quantity of electricity is passed through several electrolytes, the mass of the substances deposited are proportional to their respective chemical equivalent or equivalent weight [17].

The first law can be expressed in a mathematical form as follows:

$$V_g = \left(\frac{R \cdot I \cdot T \cdot t}{F \cdot p \cdot z} \right) \quad (10)$$

the gas volume in liters is represented by V_g, R is the ideal gas constant equal to 0.0820577 (L·atm/mol·K), I means the current in amperes, T is the temperature in $^\circ K$, t is the time in seconds, z is the number of excess electrons and takes the value of 2 for H_2 and 4 for O_2, p represents the ambient pressure in atmospheres and F represents the Faraday constant equal to 96485.331 in C/mol.

Eq. (10) can be used to obtain the amount of hydrogen generated according to a DC current in a certain amount of time, being relevant to the operation of the fuel cell.

Note that hydrogen production through water electrolysis is a method of storing wind energy, and it is of great importance to understand that the hydrogen is fundamental to the implementation of this hybrid system, since it is the energy carrier that allows the hybrid system to work autonomously for long periods of time. The hydrogen can be stored and distributed; the only by-product of this combustion is water, so no additional pollution is generated [18].

Electrolysis has the advantages of being static, simple and able to operate for long periods without attention, while generating very pure hydrogen to be used in a fuel cell.

Considering Faraday's law of electrolysis (10) and the fact that the power required by the electrolyzer can be computed by means of the power equation $P_{el} = V_c \cdot I$, where I is the current, V_c represents the cell voltage and P_{el} is the power required for the electrolyzer, the volume of hydrogen generated from a certain amount of power can be expressed as

$$V_{H_2} = \left(\frac{P_{el} \cdot R \cdot T \cdot t}{2 \cdot F \cdot p \cdot V_c} \right) \quad (11)$$

V_{H_2} is the volume of hydrogen produced by the cell. Implementing (11) the volume of hydrogen produced by the electrolyzer with P_{el} input power is deduced. Considering that the model applied to the HS will calculate the power required for the electrolyzer in the function of the wind power forecast, Eq. (11) is reorganized as

$$V_{H_2} = P_{el} \cdot l_{el} \quad (12)$$

where $l_{el} = \frac{R \cdot T \cdot t}{2 \cdot F \cdot p \cdot V_c}$.

2.3. Fuel cell model

The proton exchange membrane fuel cell (PEMFC), Fig. 2 is the type of cell that was used to develop the model, and is characterized by an efficient production of energy with high power density. Since the cell separator is a polymer tape the cell operates at a relatively low temperature, which potentially allows quick start-up and issues such as sealing, assembly and operation are less complex than in other cell types. The need for handling corrosive acids or bases in this system is removed [19].

The cell has internal electrical losses such as ohmic, mass transport and activation [20]. These internal losses in the fuel cell are neglected in this model, because their values tends to be very small and therefore do not significantly alter the result, as demonstrated in [21].

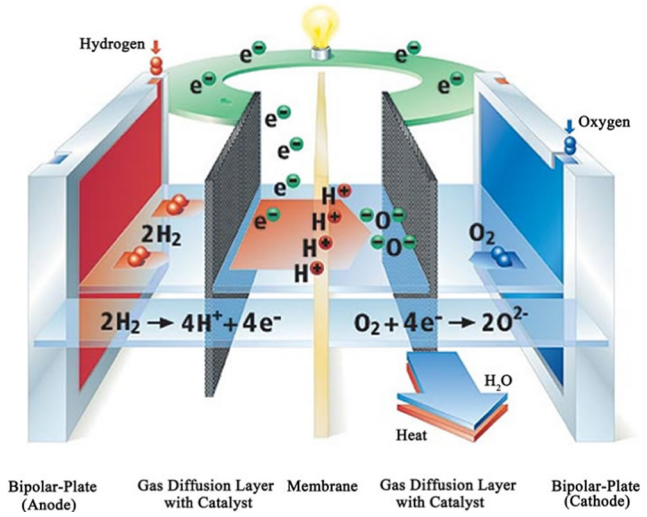

Fig. 2. Schematic of representative PEMFC.

The cell voltage, Eq. (13), is calculated based on the reversible open circuit voltage E and the voltage losses, as follows:

$$V_c = E - \Delta V_{ohm} - \Delta V_{act} - \Delta V_{trans}. \quad (13)$$

For the cell voltage, a value between 0.6 V and 0.7 V can be assumed [22]. In this research, a value of 0.68 is assumed in accordance with the efficiency of the FC.

The operation of the fuel cell can be understood to be essentially the reverse process of electrolysis of water, as this technology recombines the hydrogen with oxygen to generate electrical power and water.

To know the amount of hydrogen needed by the fuel cell, one must know the number of fuel cells that make up the stack of the final FC array. The hydrogen used by the stack, in mol/s [20,23], is given by

$$H_{2used} = \frac{P_{fc} \cdot n}{2 \cdot V_c \cdot F} \quad (14)$$

another way to calculate the hydrogen used is in kg/s, while considering the molar mass of the hydrogen and the Faraday constant (F), deduced as

$$H_{2used} = l_{fc} \cdot P_{fc} \quad (15)$$

l_{fc} is determined by $1.05 \times 10^{-8} \frac{n}{V_c}$.

In order to design the model predictive control (MPC), the impulse response function for the fuel cell is needed. Taking into account that the FC is an electrochemistry element, its dynamic is very fast as demonstrated in [24,25]. To compute the impulse response of the FC the function in Fig. 3 is implemented to obtain $l_{fc,k}$ for future used in the MPC. The same function is required to obtain the impulse response for the electrolyzer and storage, $l_{el,k}$, and $l_{st,k}$ respectively.

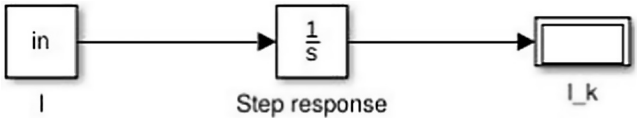

Fig. 3. Step response function.

2.4. Hybrid system setup and predictive control

The hybrid system is composed by a 5 kW Iskra wind turbine [26], a 2.4 kW PEMFC [27], an electrolyzer from the brand Proton OnSite with a net production rate of 18.8 standard litre per minute [28] and a hydrogen storage of 16,500 l [29]. The control is recreated in a computational form, in which the HS output is reflected in the activation, the power regulation and the interaction between the elements as seen in Fig. 4, where the continuous, dashed and pointed arrows represent the electric, control data, and hydrogen flow respectively. The HS is supposed to connect to the network at distribution level, taking into account the power level used by normal households in Mexico City at different times of the year [30]. The HS can be adjusted to work as a constant power generator or to meet a signal reference output power, based on the daily historic load of the household(s). This can make the user change his or her consumption habits in order to have a better response to the system and to decrease the total cost of their electric consumption [31,32].

Fig. 4 shows the flow of the main energies that sustain the HS where the left side is the hydrogen flow and the right side is the electric power flow with the input and outputs of the systems. This figure also shows the electric conversion AC/DC and DC/AC taking into account that the FC has a DC output. The power will be controlled, regulated and distributed to the network and electrolyzer with the purpose of storing energy in the form of hydrogen.

Depending on the objective function, various MPC strategies can be implemented. MPC has the inherent advantages like the use for controlling a great variety of processes, including systems with long delay times or of non-minimum phases or unstable ones [33,34]. In addition, the MPC introduces feedforward control to compensate measurable disturbances, allowing its application to this work to be more satisfactory [35].

Fig. 5 shows the basic structure of MPC; the future outputs for a horizon N are predicted at each instant t. The predicted outputs for $k = 1, \ldots, N$ depend on the known values up to instant t and on the future control signals, $k = 0, \ldots, N-1$, which are to be sent to the system. The future control signals are calculated by optimizing a criterion in order to keep the process close to the reference trajectory $P^{ref}_{t+k|t}$, which is computed as the result of

$$P_{t+k|t} = \widehat{P}^{w}_{t+k|t} + P_{fcmax,k} - P_{elmax,k} \quad (16)$$

$\widehat{P}^{w}_{t+k|t}$ represents the forecasted wind power, P_{fcmax} is the activation vector of the FC and P_{elmax} is the activation vector of the electrolyzer, where the last two are computed according to the priority given in

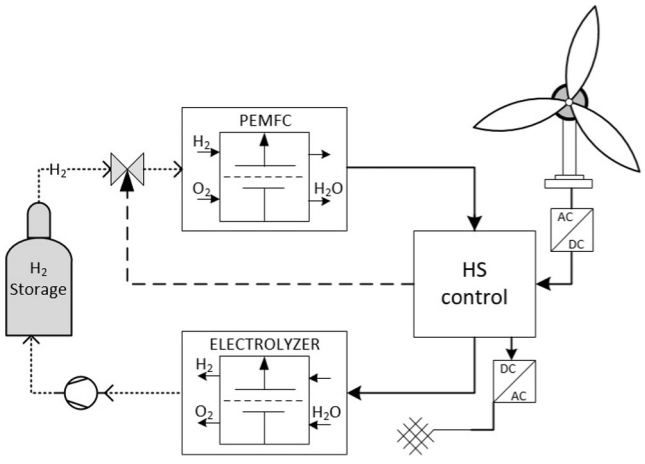

Fig. 4. Hybrid system.

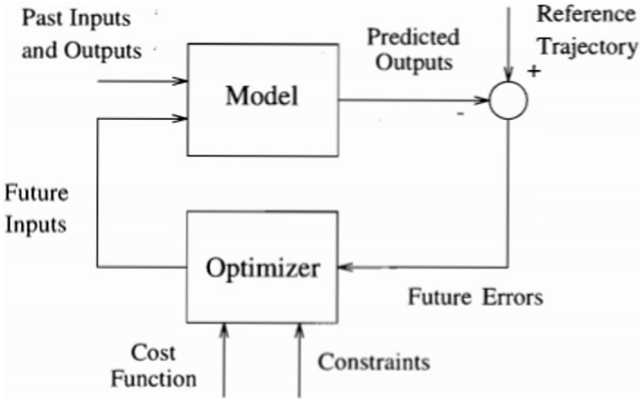

Fig. 5. Structure of MPC.

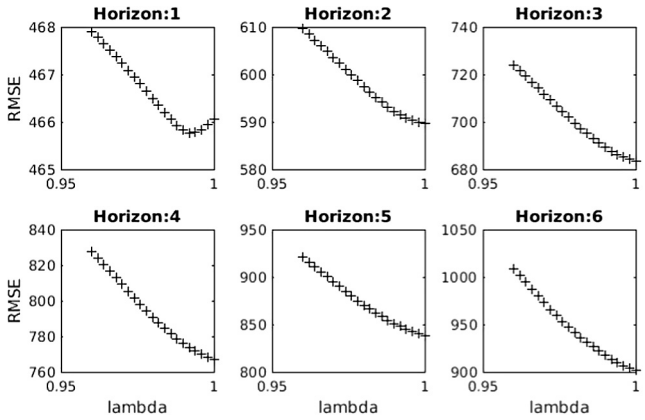

Fig. 6. Optimal forgetting factor.

the different scenarios. Eq. (16) is then filtered through a moving average filter, which operates by averaging a number of points from the input signal to produce each point in the output signal [36]. In equation form it is written as

$$P^{ref}_{t+k|t}[k] = \frac{1}{M}\sum_{j=0}^{M-1} P_{t+k|t}[k+j] \tag{17}$$

M is the number of points in the average. Afterward, $P^{ref}_{t+6|t}$ is reported, and $P^{ref}_{t+k|t}$ for $k = 1,\ldots,N$ is used in the MPC.

Taking into account the activation vector of the FC and electrolyzer depending on the priority given in the behavior of the HS, $P_{t+k|t}$ is computed. Afterward, the forecast signal is filtered as to remove the high frequency changes and leave a smooth signal to be used as the reference trajectory.

The MPC manages the electric power of the HS and takes into account the output power, the filtered forecast and the actual wind power, so that the control decides how much power the FC is going to produce and how much power will be directed to the electrolyzer for saving energy for future fluctuations, thus, the output power will be almost without frequency changes and minimizing in a great extent the intermittence and variability of the wind power.

3. Forecast and MPC implementation in the management of the hybrid system

The purpose is to report to the ISO how much power will be delivered to the grid one hour ahead.

Along the scenarios a priority is given and a constraint or condition will be added to compute $P_{t+k|t}$, changing the characteristics from Eq. (16) and recreating $P^{ref}_{t+k|t}$.

The reported data will be the trajectory followed by the HS by means of the MPC and will have the principal characteristic of being smooth in time as to avoid any operational instability like voltage or frequency in the grid because of the influence of the wind power. Furthermore, when a trajectory is applied to the control of the HS and successfully reached, it can be demonstrated that wind power as non-dispatchable energy, when implemented in a HS, can be converted to a semi-dispatchable electric source, making the management and distribution of energy more flexible.

Initially an algorithm to find the optimal forgetting factor by simply fitting a sequence of λ from 0.96 to 1 was implemented, and the value of λ which minimized the root mean square error (RMSE) was found for each horizon and forecast, as seen in Fig. 6.

The aforementioned optimal λ is implemented to compute the forecast for the different horizons applying RLS with the forgetting factor as explained in Section 2.1.2, which results in the forecast for the different horizons k as shown in Fig. 7. The algorithm implemented to forecast one hour ahead, with a resolution of 10 min, is called a six-steps-ahead forecast.

The time-series models are updated in each iteration of the process as described later in this section, taking into account the new data measured every 10 min. The expressions obtained for each horizon ($k = 1,\ldots,6$) are

$$Y_t = 161.2 + 0.8324Y_{t-1} + 0.0461Y_{t-2} \tag{18}$$

$$Y_{t+1} = 248.3 + 0.8275Y_t - 0.00922Y_{t-1} \tag{19}$$

$$Y_{t+2} = 342.65 + 0.8228Y_{t+1} - 0.0698Y_t \tag{20}$$

$$Y_{t+3} = 439.93 + 0.7703Y_{t+2} - 0.0835Y_{t+1} \tag{21}$$

$$Y_{t+4} = 525.09 + 0.6905Y_{t+3} - 0.0641Y_{t+2} \tag{22}$$

$$Y_{t+5} = 634.7 + 0.7555Y_{t+4} - 0.1978Y_{t+3}. \tag{23}$$

The result of the short term forecast together with the analysis of the ACF (Fig. 8) indicates that the used model is suitable for this study purpose.

Fig. 9 shows the RMSE as a function of the horizon k (10-min steps). The black is the RMSE for persistence and the red is for RLS. It is observed some improvement of the RLS over the persistence, but it is beyond the scope of the study to investigate the impact of using the forecasts compared to persistence.

The forecast is done using the following steps which are repeated every 10 min

- Update historic data
- Run one-hour-ahead forecast
- Compute the 'new trajectory'
- Update the 'last trajectory', adding the last 10 min of the 'new trajectory' at the end of the last one, as to always have a one-hour-ahead forecast generation
- Report the new one hour ahead updated trajectory to the ISO.

Different control scenarios were tested to be applied in the interaction of the inner elements of the hybrid system with a variety of priorities for the output power.

This section presents and explains the different scenarios of control with the more significant outputs within the ones implemented, and based on these scenarios a decision about which

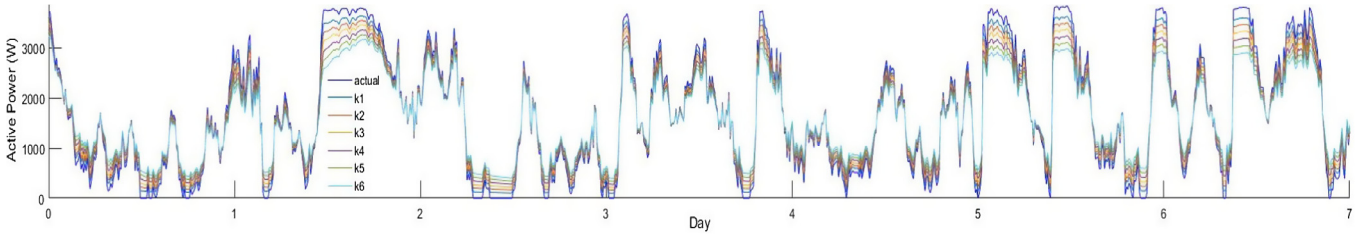

Fig. 7. Actual and k-step ahead forecast.

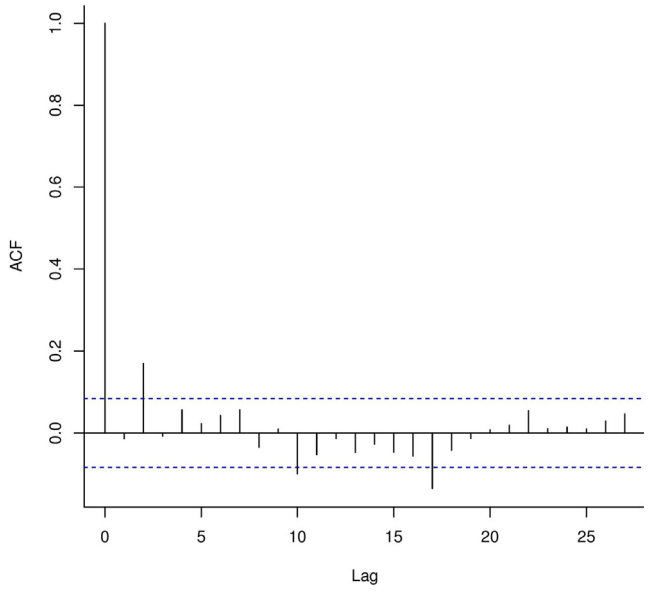

Fig. 8. ACF of the residuals.

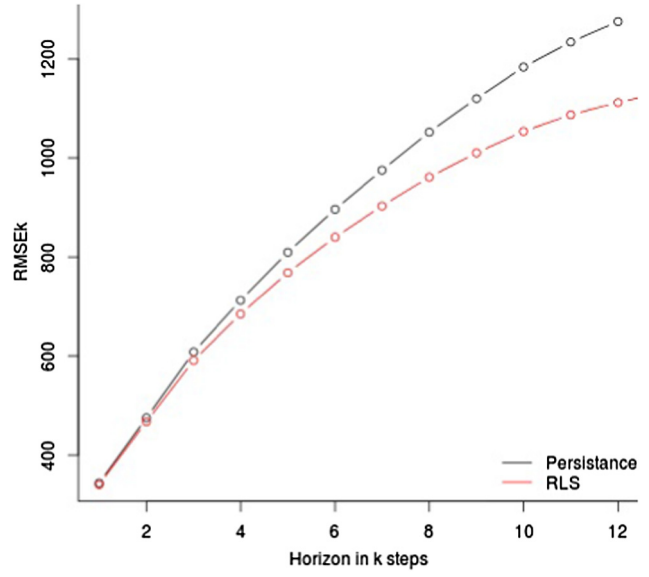

Fig. 9. RMSE as function of the horizon.

one is more convenient to implement can be taken, depending on the purpose of the HS, the priorities and needed output power.

The computational process for all scenarios is shown in Fig. 10 in a generalized way, where the constrains change in their decision making depending on the priority for the HS of the case.

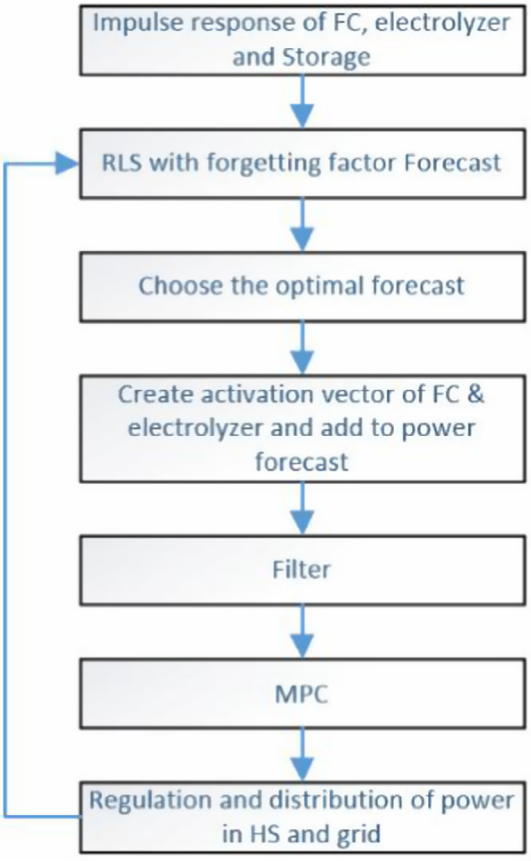

Fig. 10. HS operation flowchart.

With the computed forecast and the application of the models for the different elements that integrate the HS, the objective function can be deduced and implemented to be minimized in the MPC

$$\begin{aligned} \underset{P_{\phi,k}}{minimize} \quad & \left\| P_{w,k} - P^{ref}_{t+k|t,k} + P_{\phi,k} \right\| \\ subject\ to \quad & \phi = \textstyle\sum_{k=0}^{N} - l_{fc} P_{fc,k} + l_{el} P_{el,k} + l_{st,k} \phi_0 \\ & \phi_{min} \leqslant \phi \leqslant \phi_{max} \\ & -P^{nom}_{ele} \leqslant P_{\phi,k} \leqslant P^{nom}_{fc} \\ & P_{\phi,k} = P_{fc,k} - P_{el,k} \\ & 0 \leqslant P_{el,k} \\ & 0 \leqslant P_{fc,k}. \end{aligned} \tag{24}$$

the MPC minimizes an object function subjected to constrains and manages the power flow of the HS, where $\| \|$ is the vector norm or ℓ^2-norm, P_ϕ is the power flow to/from the elements connected to the storage calculated by the MPC, $P^{ref}_{t+k|t}$ is the reference trajectory based on the forecasted wind power computed with (17), P_{fc}

is the power to be generated by the FC, P_{el} is the power destined to the electrolyzer, ϕ represents the level of storage and ϕ_0 represents the last measure of H_2 stored, ϕ_{max} and ϕ_{min} are the physical limits of the storage, l_{el}, l_{fc} and l_{st} represent the impulse response of the electrolyzer, FC and storage respectively based on the aforementioned models.

The constraints for the FC and electrolyzer are vectors with the physical nominal values of the elements represented by P_{fc}^{nom} and P_{ele}^{nom} respectively and implemented in the MPC. $P_{w,k}$ represents the vector with the actual power $(k=0)$ and forecasted wind power $(k=1,\ldots,N)$ meaning $P_w=\left[P_{k=0},\widehat{P}^w_{t+k|t}\right]$. For a better understanding of P_w Fig. 11 is required, where $t=27$ h 30 min represents the actual instant, which is the $k=0$ point. The continuous line before the $k=0$ point is the historic data incorporated in the time series analysis, and the dashed line after $k=0$ is the hour-ahead forecast representing the $k=1$ until $k=6$ steps-ahead, forecast based on the historic data and including the actual data at $k=0$, mentioned in Sections 2.1 and 3.

4. Different scenarios for the management system

Immediately afterward, two scenarios are implemented to validate the algorithm proposed in this paper. The scenarios contain certain priorities and have the main purpose of zero network frequency disturbance and as a second purpose, possesion of a more stable and semi-dispatchable power generation.

The first scenario is tasked with just smoothing the wind power, in Fig. 12, by implementing the power generated by the FC and the MPC as a controller, which is prioritized this way to analyze the response of the HS. The second scenario focuses on having a more linearized output power from the HS and the possible "sacrifices" to accomplish it.

4.1. Smoothing the wind power

In this scenario, the priority is to smooth the wind power generated by the turbine, controlling the output power of the HS at every moment. To compute $P^{ref}_{t+k|t}$ from (16), first one must calculate P_{elmax} and P_{fcmax} considering the restrictions of the electrolyzer and FC.

To calculate the vector P_{elmax}, both physical and characteristic constraints for the scenario are considered. In this scenario, the hydrogen level in the tank will be at least lower than an upper threshold (Γ_{elup}) level when charging or until the maximum of the tank is reached because of surplus of wind power, and above a lower threshold (Γ_{eldown}) of the tank, described mathematically as

$$P_{elmax}=\begin{cases}\widehat{P}^w_{t+k|t} & \phi \leqq \phi_{max}\Gamma_{elup}\\ 0 & \phi > \phi_{max}\Gamma_{elup}\end{cases} |\phi \leqq \phi_{max}\Gamma_{eldown}. \tag{25}$$

the hydrogen storage will be charged when the tank presents a specified level of hydrogen, represented by the lower threshold (Γ_{eldown}), bearing in mind a base amount of hydrogen in case of contingency because of the uncertainty of the wind speed. The base amount will be assumed as the hydrogen required to generate maximum power from the FC in the next two hours, ensuring a smooth change in the output power without affecting the frequency of the network. In the charging period, the electrolyzer will use the wind power to produce hydrogen until the storage level reaches a specified upper threshold (Γ_{elup}) in which it stops charging. In this paper, Γ_{elup} represents the hydrogen required for the FC to work eight hours ahead at maximum power.

Storage plays a great role when it comes to maintaining a stable output power of the HS for long periods of time. The activation and deactivation of the electrolyzer is the principal factor for mantaining a level of storage. As seen in Fig. 13 a global flow chart explains how it was applied in the model, giving an idea of how it can be modified depending on the priority of the storage required from the HS.

To ensure constant smooth output power from the HS, constraints were applied on the activation of the FC. As a result the FC generates more frequently and compensates the variability in the wind power, according to the amount of hydrogen stored. When there is no wind, the output power is determined by the nominal FC value. Given the uncertainty in the wind speed this constraint was necessary to attain the designated power value without having to ask for backup from the grid. Therefore, the nominal value of the FC must be implemented in the MPC and in the activation of the FC. To compute $P^{ref}_{t+k|t}$ from (25), the activation vector of the FC is then calculated by

$$P_{fcmax}=\begin{cases}P^{nom}_{fc}-\widehat{P}^w_{t+k|t} & P_{fcmax,k}>0\\ 0 & P_{fcmax,k}\leqq 0\end{cases} |\phi_{max}\Gamma_{fc} \leqslant \phi \tag{26}$$

the nominal power of the FC is represented by P^{nom}_{fc}, and Γ_{fc} is the threshold of minimum percent of hydrogen stored for the FC to generate power; in case that the threshold cannot be met, the value of P_{fcmax} will be zero. Furthermore, P_{fcmax} is computed taking into account P^{nom}_{fc} to ensure that the max value asked from the FC will not be greater than the nominal power of the FC and to help linearize the output power of the HS.

The maximum power of the HS in this scenario will be determined as the sum of the wind power and the power from the FC given by $P_{fc,k}=P^{nom}_{fc}-\widehat{P}^w_{t+k|t}$.

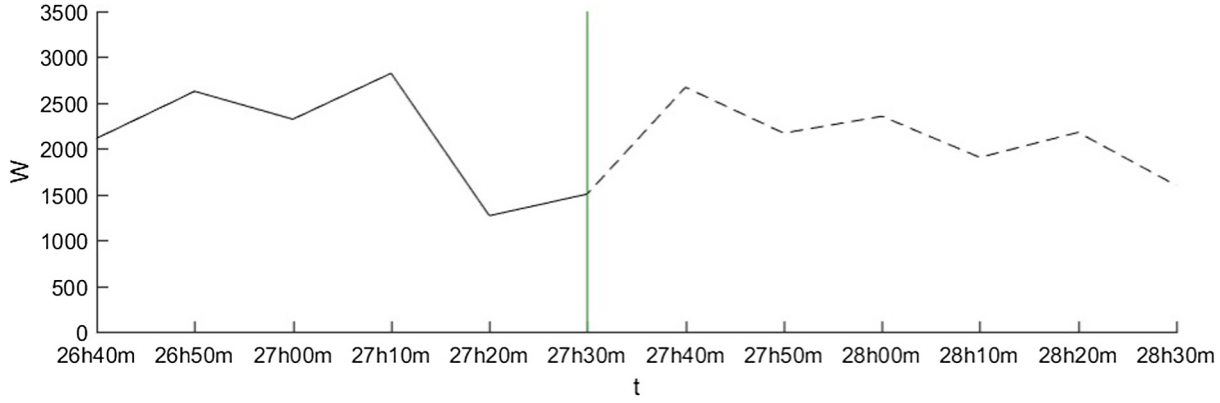

Fig. 11. Forecast at $t=27$ h 30 min.

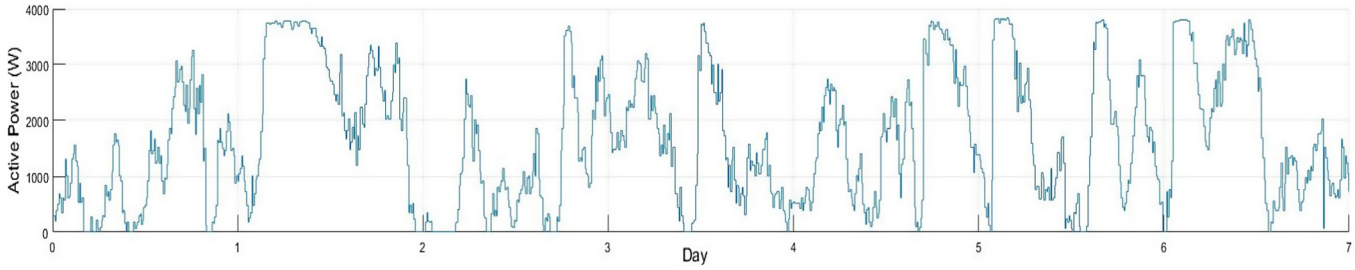

Fig. 12. Actual wind power.

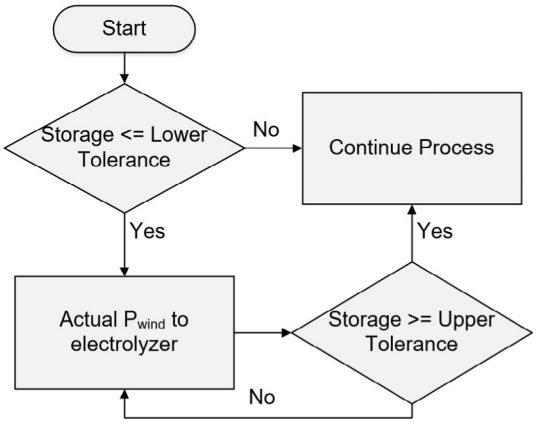

Fig. 13. Activation of electrolyzer.

The sum of the power generated by the FC and forecast for the wind turbine will be filtered using (17) which will smooth the flickers, resulting in the reference for the MPC (24); simultaneously, this reference will be the output power of the HS.

4.2. Prioritizing stable output power level of the hybrid system

When the priority is to have a more stable output power from the HS, the resulting analysis of the previous scenario is of great importance. Because of the intermittence of wind speed, the appearance of many sags in the power forecast and actual power is common. To maintain a linear output power means the need to "sacrifice" other characteristics as, in this case, the magnitude of power supplied from the HS to the distribution network given by

$$P^{ref}_{t+k|t}[k] = \frac{a}{M}\sum_{j=0}^{M-1} P_{t+k|t}[k+j] \tag{27}$$

where a will take values between 0 and 1.

In this scenario, the filter at the control part of the model was modified from Eq. (17) as to have more energy stored and to decrease the output magnitude to 60% ($a = 0.6$) of the original power value. Thus the residual 40% will be supplied to the electrolyzer and consequently will generate hydrogen to store. The updated filtered signal will be the output power of the HS for the next hour.

5. Results and discussion

Each subsection from Section 4 focuses on the required characteristics needed to smooth and flatten the output power of the HS in order to overcome the intermittence of wind power.

When the HS is connected to the network, it will not destabilize the frequency as demostrated in this section. The obtained results show the first week behavior of the HS, for the reader to notice in a clear way the dispatchability and reduction of intermittence in comparison to a system without the application of the proposed model as the actual wind power.

5.1. Active power delivered from the HS

The designed HS system is to be connected to the distribution network as mentioned before. From results, it can be seen how the unpredictability from the wind power (Fig. 12) is solved as shown in the HS output power obtained with the proposed AEMS model (Fig. 14a). The network frequency will not be affected considering that the HS output power can be dispatched according to the final user needs and the information can be sent to the ISO with one hour prior.

Fig. 14a presents the HS output power for both scenarios. Results from the first scenario show that because of the periods of charge, the HS output power has periods of no power delivered to the network, the implementation of the constraints required to activate the electrolyzer, are also the moments of no power generated by the HS resulting from the electrolyzer consuming all the power generated by the wind turbine with the purpose of storing energy as hydrogen. Note in Fig. 14a that the response obtained from the second scenario, when compared to the first scenario, is flatter, more stable and more constant as it was expected.

Observing the results of the different scenarios, the HS output power can be adjusted to meet a specific load which modifies the trajectory followed by the MPC and the constraints applied. In addition, because of the flexibility of the MPC, the constraints that rule the charge and discharge of the hydrogen storage can be modified considering the purpose of the HS.

The reduction of volatility of the power delivered to the distribution network is noticeable, comparing the wind power from Fig. 12 and the output power of the HS from Fig. 14a.

The output power of the HS is the sum of wind power with the power generated by the FC, as shown in Fig. 15, where the color at the base represents the power delivered from the wind turbine, and the color on top is the power delivered by the FC, showing how the wind power and FC complement each other.

5.2. Hydrogen storage behavior

The behavior of the hydrogen generated by the electrolyzer and consumed by the FC in the different scenarios can be seen in Fig. 14b, where it can be noticed that when the electrolyzer works the hydrogen tank is charged and when the FC works the storage level of hydrogen will decrease.

The storage constantly maintains a minimum level of hydrogen as shown in Fig. 14b; thanks to this, the FC can work longer permitting a smooth or flat output from the HS.

Comparing the production and consumption of hydrogen from both scenarios, results show that there is 1.74% less production

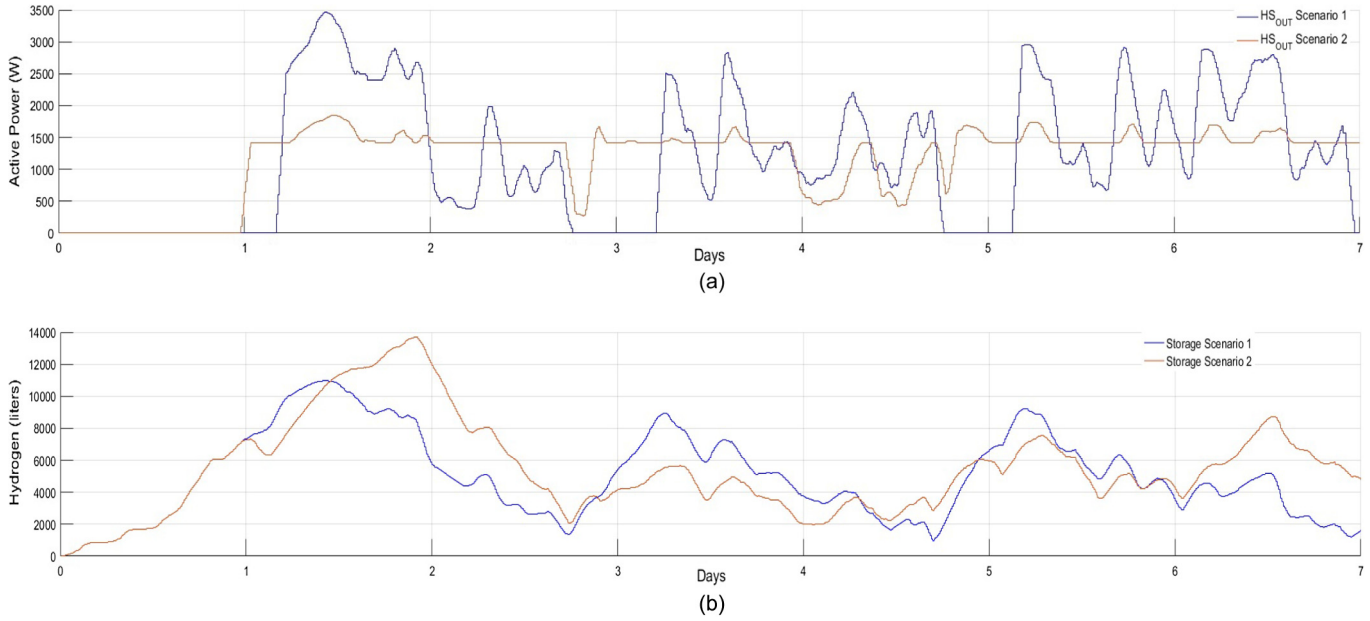

Fig. 14. (a) Total power generated by the HS in both scenarios. (b) Behavior of hydrogen storage in the different scenarios.

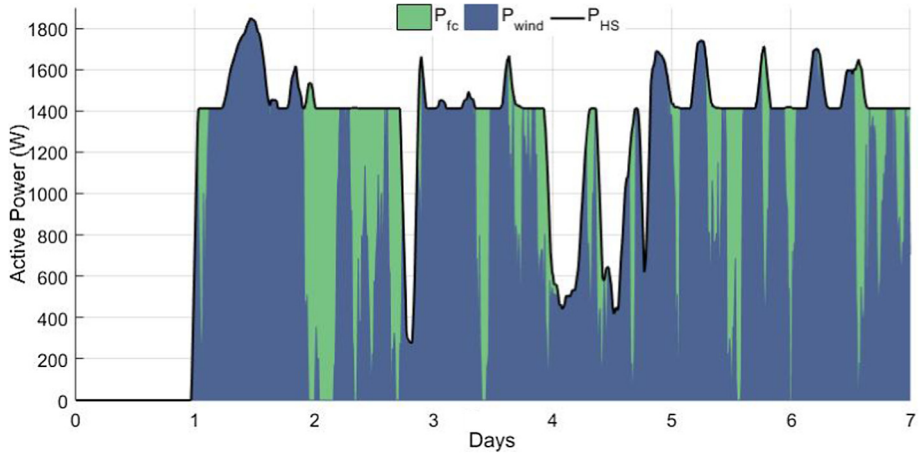

Fig. 15. Resources dispatch of the P_{HS} delivered to the grid.

of H_2 and 9.93% less consumption of it in the second scenario at the end of the week. However, the storage of the second scenario presents 17.65% more hydrogen in comparison with the first scenario where it is almost empty as seen in Fig. 14b. These results are caused by the level of power required in each scenario. The second delivers a lower level of active power to possess a more constant output at all time, in contrast to the first scenario, which due to the level of power delivered needs periods of zero output power as to generate H_2 to storage.

The storage from the first scenario always has a good level of hydrogen ready to be used by the FC in a more efficient way as in Fig. 14b, but clearly because of the charging periods of hydrogen, the output power drops to zero at the output of the HS.

The hydrogen consumption is constant, and therefore, the tank will not reach a high level of storage, tending instead to maintain a lower mean of hydrogen, as shown in Fig. 14b.

5.3. Findings of the method

Taking into account the importance of charging periods for the storage of hydrogen and of keeping an output power level as linear as possible, decreasing the output power level to generate hydrogen was required for longer periods of time and for the FC to work as backup power to have an almost linearized power level at the output of the HS.

The FC can act as a means of contingency to smooth the output power thanks to the hydrogen stored in the tank, and because of the decision making based on the forecast that gives information about future possible fast changes in wind power, it is possible the use of the FC as a measure for preventing disturbance of the frequency of the network.

The surplus of energy from the high peaks of wind power is saved as hydrogen for future implementation, making smooth wind power and semi-dispatchable HS generated power possible.

6. Conclusions

One of the most important conclusions is the fact that wind power as a non-dispatchable kind of energy, when employed in a hybrid system with implementation of forecast, can be managed as a semi-dispatchable energy. The generation can be modeled based on the needs of the end user or as a base energy for long periods of time, depending on the capacity of the storage and output power required for the system. Consequently, the frequency of the system will not be compromised because of sudden changes in wind power. The proposed HS is meant to work in the distribution level for housing sectors and small stores.

In real life application, this HS model will help to keep the net frequency in the tolerance rate, given the fact that it will not be disturbed by the HS when connected as DG into the network, thanks to the no uncertainty and no intermittence in the HS output power.

When the priority is completely given to the FC generation, there is a high risk of running out of hydrogen and not meeting the full capacity of the HS.

Another finding is the fact that to generate a completely linear power output, there is a need to "sacrifice" other features such as magnitude power, storage limits and even the times to recharge the hydrogen tank according to the needs of the end user; hence, it is recommended to compromise the involved parties regarding the HS.

The implementation of forecast is demonstrated to be of great importance in planning the dispatch of power, improving and taking contingency measurements as to avoid disturbing the network or even improving the network in the connection point if necessary.

Forecast applied to wind power and used for the MPC allows the manipulation of the elements that make the HS obtain the desired output power while avoiding penalties.

Acknowledgments

M.F.A.M gratefully acknowledges the support of DTU-Compute and appreciates the financial support of the CITIES project, supplementary to CONACyT-Mexico through a doctoral grant (CVU 595035).

References

[1] Zhang H, Xing F, Cui H-Z, Chen D-Z, Ouyang X, Xu S-Z, et al. A novel phase-change cement composite for thermal energy storage: fabrication, thermal and mechanical properties. Appl Energy 2016;170:130–9. http://dx.doi.org/10.1016/j.apenergy.2016.02.091. ISSN 0306-2619.

[2] Bagen, Billinton R. Evaluation of different operating strategies in small stand-alone power systems. IEEE Trans Energy Convers 2005;20(3):654–60. http://dx.doi.org/10.1109/TEC.2005.847996. ISSN 0885-8969.

[3] Ma T, Yang H, Lu L. Performance evaluation of a stand-alone photovoltaic system on an isolated island in Hong Kong. Appl Energy 2013;112:663–72. http://dx.doi.org/10.1016/j.apenergy.2012.12.004. ISSN 0306-2619.

[4] Bouffard F, Galiana FD. Stochastic security for operations planning with significant wind power generation; 2008. p. 1–11. http://dx.doi.org/10.1109/PES.2008.4596307.

[5] Zhao Y, Ye L, Li Z, Song X, Lang Y, Su J. A novel bidirectional mechanism based on time series model for wind power forecasting. Appl Energy 2016;177:793–803. http://dx.doi.org/10.1016/j.apenergy.2016.03.096. ISSN 0306-2619.

[6] Wang J, Botterud A, Bessa R, Keko H, Carvalho L, Issicaba D, et al. Wind power forecasting uncertainty and unit commitment. Appl Energy 2011;88(11):4014–23. http://dx.doi.org/10.1016/j.apenergy.2011.04.011. ISSN 0306-2619.

[7] Bathurst GN, Strbac G. Value of combining energy storage and wind in short-term energy and balancing markets. Electr Power Syst Res 2003;67(1):1–8. http://dx.doi.org/10.1016/S0378-7796(03)00050-6. ISSN 0378-7796.

[8] Exizidis L, Kazempour SJ, Pinson P, de Greve Z, Vallée F. Sharing wind power forecasts in electricity markets: a numerical analysis. Appl Energy 2016;176:65–73. http://dx.doi.org/10.1016/j.apenergy.2016.05.052. ISSN 0306-2619.

[9] Fathima AH, Palanisamy K. Optimization in microgrids with hybrid energy systems – a review. Renew Sustain Energy Rev 2015;45:431–46. http://dx.doi.org/10.1016/j.rser.2015.01.059. ISSN 1364-0321.

[10] McKenna R, Hollnaicher S, Fichtner W. Cost-potential curves for onshore wind energy: a high-resolution analysis for Germany. Appl Energy 2014;115:103–15. http://dx.doi.org/10.1016/j.apenergy.2013.10.030. ISSN 0306-2619.

[11] Santamaría-Bonfil G, Reyes-Ballesteros A, Gershenson C. Wind speed forecasting for wind farms: a method based on support vector regression. Renew Energy 2016;85:790–809. http://dx.doi.org/10.1016/j.renene.2015.07.004. ISSN 0960-1481.

[12] Box GEP, Jenkins GM, Reinsel GC. Time series analysis. Hoboken, NJ: John Wiley & Sons, Inc.; 2008. http://dx.doi.org/10.1002/9781118619193. ISBN 9781118619193.

[13] Hastie T, Tibshirani R, Friedman J. The elements of statistical learning. Springer series in statistics. New York, NY: Springer New York; 2009. http://dx.doi.org/10.1007/978-0-387-84858-7. ISBN 978-0-387-84857-0.

[14] Madsen H. Time series analysis. Chapman & Hall/CRC; 2008. ISBN 9781420059670.

[15] Rasmussen LB, Bacher P, Madsen H, Nielsen HA, Heerup C, Green T. Load forecasting of supermarket refrigeration. Appl Energy 2016;163:32–40. http://dx.doi.org/10.1016/j.apenergy.2015.10.046. ISSN 03062619.

[16] Santos DMF, Sequeira CAC, Figueiredo JL. Hydrogen production by alkaline water electrolysis. Química Nova 2013;36(8):1176–93. http://dx.doi.org/10.1590/S0100-40422013000800017. ISSN 0100-4042.

[17] Ehl RG, Ihde AJ. Faraday's electrochemical laws and the determination of equivalent weights. J Chem Educ 1954;31(5):226. http://dx.doi.org/10.1021/ed031p226. ISSN 0021-9584.

[18] Twidell J, Weir AD. Renewable energy resources. Taylor & Francis; 2006. ISBN 0419253300.

[19] I. EG&G Technical Services, Fuel Cell Handbook, U.S. Department of Energy, seventh ed.; 2004. ISBN 9781365101137.

[20] Kunusch C, Puleston P, Mayosky M. Sliding-mode control of PEM fuel cells. Advances in industrial control. London: Springer London; 2012. http://dx.doi.org/10.1007/978-1-4471-2431-3. ISBN 978-1-4471-2430-6.

[21] Kunusch C, Puleston PF, Mayosky MA, Moré JJ. Characterization and experimental results in PEM fuel cell electrical behaviour. Int J Hydrogen Energy 2010;35(11):5876–81. http://dx.doi.org/10.1016/j.ijhydene.2009.12.123. ISSN 03603199.

[22] Larminie J, Dicks A. Fuel cell systems explained. 2nd ed. J. Wiley; 2003. ISBN 9780470848579.

[23] Sammes N, editor. Fuel cell technology, engineering materials and processes. London: Springer London; 2006. http://dx.doi.org/10.1007/1-84628-207-1. ISBN 978-1-85233-974-6.

[24] Yan Q, Toghiani H, Causey H. Steady state and dynamic performance of proton exchange membrane fuel cells (PEMFCs) under various operating conditions and load changes. J Power Sources 2006;161(1):492–502. http://dx.doi.org/10.1016/j.jpowsour.2006.03.077. ISSN 0378-7753.

[25] Kannan A, Kabza A, Scholta J. Long term testing of start-stop cycles on high temperature PEM fuel cell stack. J Power Sources 2015;277:312–6. http://dx.doi.org/10.1016/j.jpowsour.2014.11.115. ISSN 0378-7753.

[26] Catalogue of European Urban Wind Turbine Manufacturers potx. <http://123doc.org/document/1227748-catalogue-of-european-urban-wind-turbine-manufacturers-potx.htm> [accessed: 2016-11-01].

[27] FCgen-1300 - Ballard - PDF Catalogue—Technical Documentation—Brochure. <http://pdf.directindustry.com/pdf/ballard/fcgen-1300/22779-383681.html> [accessed: 2016-11-01].

[28] Electrolyzer specifications S20, S40. <http://protononsite.com/products/s10-s20-s40> [accessed: 2016-11-01].

[29] HBank technologies - fuel cell application. <http://www.hbank.com.tw/fc/16500.html> [accessed: 2016-11-01].

[30] Ramos Niembro G, Sada Gámiz J, Buitrón Sánchez Horacio. Variables que influyen en el consumo de energía eléctrica, boletín iie 23.

[31] Jiang L, Luo S, Li J. Intelligent electrical event recognition on general household power appliances. In: 2014 IEEE 15th workshop on control and modeling for power electronics (COMPEL). IEEE; 2014. p. 1–3. http://dx.doi.org/10.1109/COMPEL.2014.6877183. ISBN 978-1-4799-2147-8.

[32] Mohsenian-Rad AH, Wong VWS, Jatskevich J, Schober R, Leon-Garcia A. Autonomous demand-side management based on game-theoretic energy consumption scheduling for the future smart grid. IEEE Trans Smart Grid 2010;1(3):320–31. http://dx.doi.org/10.1109/TSG.2010.2089069. ISSN 1949-3053.

[33] Camacho EF, Bordons C, Grimble MJ, Johnson MA. Model predictive control. Advanced textbooks in control and signal processing. London: Springer London; 2007. ISBN 978-1-85233-694-3 978-0-85729-398-5.

[34] Halvgaard R, Poulsen NK, Madsen H, Jorgensen JB, Marra F, Bondy DEM. Electric vehicle charge planning using economic model predictive control. In: 2012 IEEE international electric vehicle conference. IEE; 2012. p. 1–6. http://dx.doi.org/10.1109/IEVC.2012.6183173. ISBN 978-1-4673-1561-6.

[35] Maciejowski J. Predictive control with constraints. Harlow, England; New York: Prentice Hall; 2002. ISBN 978-0-201-39823-6.

[36] Smith SW. The scientist and engineer's guide to digital signal processing. California Technical Pub; 1997. ISBN 0966017633.